Novel 2-Dimensionally Periodic Non-Constant Mean Curvature Morphologies of 3-Miktoarm Star Terpolymers of Styrene, Isoprene, and Methyl Methacrylate

Stella Sioula,[†] Nikos Hadjichristidis,[†] and Edwin L. Thomas*[,‡]

Department of Chemistry, University of Athens, Panepistimiopolis, 15771 Zografou, Athens, Greece, and Department of Materials Science, Massachusetts Institute of Technology, Cambridge, Massachusetts 02139

Received December 22, 1997; Revised Manuscript Received March 25, 1998

ABSTRACT: The morphology of a family of four 3-miktoarm star terpolymers of polystyrene (PS), polyisoprene (PI), and polymethyl methacrylate (PMMA) was studied. For three of the samples, the molecular weight of the PMMA block was systematically varied while that of the PS and PI blocks were held fixed. In the fourth sample, the PS and PMMA blocks were approximately of the same molecular weight and the PI was the majority component. In all terpolymers, the system displayed a three-phase, two-dimensionally periodic microstructure of an inner PI column with a surrounding PS annulus in a matrix of PMMA. For the two samples with the longer PMMA blocks (218 and 186 kg/mol), the PI−PS and PS−PMMA interfaces were cylindrical, whereas a unique nonconstant mean curvature (non-CMC) concentric diamond prism shape of the PI and PS microdomains occurred for the sample with the lowest molecular weight PMMA block (144 Kg/mol) as well as the polymer with the longer PI block. In these star terpolymers there are three chemically different chains emanating from the same junction point. The interaction parameter between PS and PMMA is relatively low, whereas that between PI and PMMA is the highest. The star molecular architecture gives the molecule the ability to "choose" which arms directly interact in the microphase segregate state. In the present systems, the junctions lie on the PI−PS interface causing partial mixing of the PS and PMMA blocks, while minimizing the highly unfavorable contact between the PI and PMMA blocks.

Introduction

Morphological studies of ABC triblock terpolymers consisting of three chemically different components have been of recent interest both experimentally[1−7] and theoretically.[8,9] In contrast to diblock copolymers consisting of two chemically different components where the composition, the interaction parameter, and the number of Kuhn segments are the main parameters that determine the equilibrium microphase morphology, the morphology of linear triblock terpolymers is governed by two independent composition variables (ϕ_A, ϕ_B, and $\phi_C = 1 - \phi_A - \phi_B$) and by three interaction parameters (χ_{AB}, χ_{AC}, and χ_{BC}). The other major factor influencing the microphase morphology is the sequence of the blocks in the chain.[1,7]

Because of synthetic difficulties, rather little attention has been given to 3-miktoarm stars of the ABC type. Fujimoto et al.[10] prepared a 3-miktoarm star of polystyrene (PS), poly(dimethylsiloxane) (PDMS), and poly(*tert*-butyl methacrylate) (PtBMA). Hückstädt et al.[11] prepared a 3-miktoarm star of PS, 1,2-polybutadiene (1,2-PB), and polymethyl methacrylate (PMMA). Hadjichristidis' group synthesized 3-miktoarm stars of PS, 1,4-polyisoprene (1,4-PI), and 1,4-polybutadiene (PB) (SIB)[12] and of PS, 1,4-PI, and PMMA (SIM).[13] Morphological studies of the SIB 3-miktoarm star showed that the two dienes are mixed because of their low interaction parameter, and the polymer exhibits only two types of compositionally distinct microdomains.[14] The morphology of the polymers prepared by Fujimoto et al.[10] was recently reported by Okamoto et al.[15] Star terpolymers of PS, PDMS, and PtBMA, with weight fraction ratio ∼1:1:1 were studied by differential scanning calorimetry (DSC), transmission electron microscopy (TEM), and small-angle X-ray scattering (SAXS). DSC indicated the system microphase separated into three microdomains. The TEM and SAXS results suggested the existence of a regular microdomain structure with a 3-fold symmetry. From the TEM images, the authors speculated that the PDMS microdomain was continuous in three dimensions. The other two phases were not distinguishable in the images. The authors hypothesized that the other two microphases were also continuous in three dimensions, but a specific microdomain model was not proposed.

In this paper we report the morphology of a series of 3-miktoarm star terpolymers comprised of PS, PI, and PMMA (SIM). In this case all materials exhibit a distinct three-phase microdomain structure. The PS and PMMA arms show a pronounced incompatibility towards PI, whereas the PS and PMMA arms are organized into a novel annulus-matrix structure. The macromolecular architecture of the stars enables the system to "choose" the contacts between the phases. As a consequence, new types of ordered microphase morphologies result.

Experimental Methods

High vacuum techniques, described elsewhere, were used for the synthesis of the 3-miktoarm star terpolymers.[13] Size exclusion chromatography (SEC) experiments were carried out at 30 °C with a Waters model 510 pump, Waters model 410 differential refractometer, and Waters model 486 tunable absorbance detector. Three Phenomenex (type: phenogel 5 linear; pore size: $50-10^6$ Å) columns were used. Tetrahydro-

[†] Department of Chemistry.
[‡] Department of Materials Science.

S0024-9297(97)01848-2 CCC: $15.00
Published on Web 07/15/1998

Table 1. Molecular Characteristics of the 3-Miktoarm Star Terpolymers (SIM)

polymer	$M_w \times 10^{-3}$ [a]	M_w/M_n [b]	PS/PI/PMMA (% wt) [c]	PS/PI/PMMA (% vol)	ϕ_1: ϕ_2: ϕ_3	$\chi_{SI}N_{SI}$	$\chi_{SM}N_{SM}$
PS arm [d]	72	1.03	—	—	—	—	—
PI arm [d]	77	1.04	—	—	—	—	—
SIM-72/77/218	367	1.10	19.6/20.9/59.5	20.5/25/54.5	1/1.2/2.7	93	50
SIM-72/77/186	335	1.11	21.5/23/55.5	22.3/27.2/50.5	1/1.2/2.3	93	45
SIM-72/77/144	293	1.07	24.6/26.3/49.1	25.3/30.7/44	1/1.2/1.7	93	36
SIM-57/85/49	191	1.06	29.8/44.5/25.6	29/49.3/21.7	1.3/2.3/1	88	18

[a] LALLS in THF at 25 °C. [b] SEC in THF at 30 °C. [c] Average from ^{1}H NMR in $CDCl_3$ at 35 °C and SEC-UV at 260 nm. [d] Same for the three star terpolymers.

furan (THF) was used as the carrier solvent at a flow rate of 1 mL/min.

The weight-average molecular weight (M_w) of the polymers was determined with a Chromatix KMX-6 low-angle laser photometer (LALLS). This instrument, equipped with a helium−neon laser, was operating at a wavelength of 633 nm. THF, distilled over CaH_2 and sodium-distilled prior to use, was the solvent at 25 °C. The refractive index increments, dn/dc in THF at 25 °C, were measured with a Chromatix KMX-16 refractometer, operating at 633 nm and calibrated with NaCl solutions. The M_w values were obtained from the $(KC/\Delta R_\theta)^{1/2}$ versus C plots (ΔR_θ, excess Rayleigh ratio; K, combination of known optical constants; C, concentration) and the correlation coefficient was >0.99.

The PI arm was analyzed by ^{1}H and ^{13}C NMR (Varian 540 Unity Plus) spectroscopy in $CDCl_3$ at 35 °C, and found to have the following microstructure: 71 wt % *cis*-1,4; 21 wt % *trans*-1,4; 8 wt % 3,4. The composition of the polymers was analyzed by ^{1}H NMR, and the PS content was also determined by SEC−UV analysis at 260 nm.

For SAXS and TEM characterization, ~0.7-mm thick films of the materials were cast from a dilute solution (~4 wt %) with chloroform [solubility parameters: $CHCl_3$: $\delta = 9.3$ (cal/cm^3)$^{1/2}$; PS: $\delta = 9.1$ (cal/cm^3)$^{1/2}$; PI: $\delta = 8.2$ (cal/cm^3)$^{1/2}$; PMMA: $\delta = 9.3$ (cal/cm^3)$^{1/2}$]. Then, the polymer films were dried for 1 day under reduced pressure at room temperature. Finally, to obtain near-equilibrium microstructures, the films were annealed for 5 days at 140 °C under reduced pressure.

The X-ray diffraction (XRD) patterns were acquired at room temperature on the Time-Resolved Diffraction Facility (station X12B) at the National Synchrotron Light Source at Brookhaven National Laboratory (BNL) with a custom-built two-dimensional detector (10 × 10 cm, 512 × 512 pixels) interfaced to a real-time histogramming memory system.[16] The optical system provides a doubly focused monochromatic X-ray beam with a wavelength (λ) of = 1.54 Å.

For TEM investigation, 500−1500-Å thick sections were cryomicrotomed at approximately −90 °C with a Reichert-Jung FC 4E cryoultramicrotome equipped with a diamond knife. Sections were picked up on 600-mesh copper grids and, to enhance mass-thickness contrast, they were placed in the vapors of a 4% osmium tetroxide-water solution for 1 h for selective staining of the diene phase or in the vapors of a 0.5% ruthenium tetroxide-water solution for 0.5 h for selective staining of the PS and PI phases. A JEOL 200CX electron microscope, operated at 200 kV and at 100 kV in the bright field mode, was used to examine the stained sections.

Fast Fourier transforms (FFT) were made from 1024 × 1024 pixel arrays of the TEM images, digitized at 600 dots per inch. A FFT program written by Dr. R. Lescanec employs a Hanning window to reduce edge effects and outputs the data on a log scale as a two-dimensional image.

Results and Discussion

The molecular characteristics and degree of segregation [$\chi_{ij}(N_i + N_j$] of the 3-miktoarm star terpolymers are given in Table 1. The nomenclature used is SIM-x/y/z, where x, y, z are the respective block molecular weights in kg/mol. The Flory−Huggins interaction parameters of PS−PMMA and PI−PS at 140 °C are estimated as ~0.017 and 0.051, respectively.[17] Based on solubility parameters of the components, the χ parameter between PI and PMMA is expected to be the highest. To ensure that all three components are microphase separated, the molecular weights of both PS and PMMA blocks were made high because the χ_{SM} is the lowest interaction parameter.

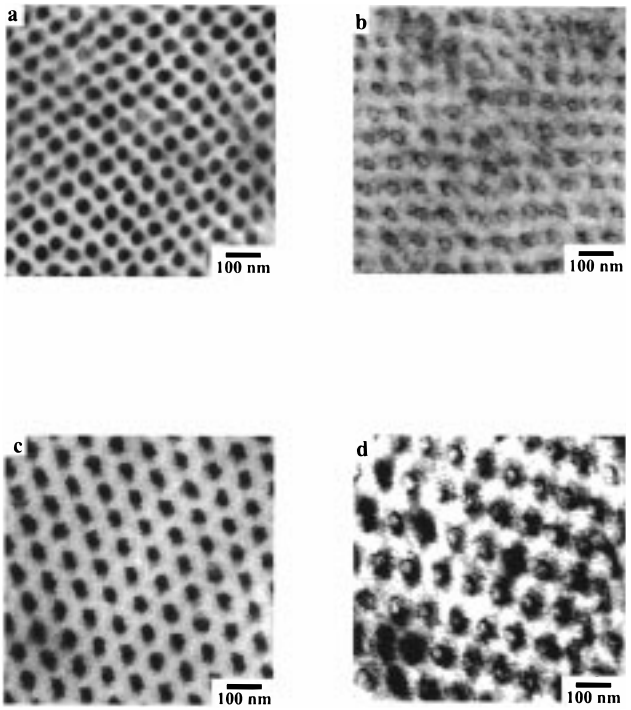

Figure 1. Bright field TEM images of (a) SIM-72/77/186 stained with OsO_4, (b) SIM-72/77/186 stained with RuO_4, (c) SIM-72/77/218 stained with OsO_4, and (d) SIM-72/77/218 stained with RuO_4. In the OsO_4 stained micrographs, the dark regions correspond to the PI phase, which forms hexagonally packed cylinders, whereas in the RuO_4 stained micrographs, the gray regions correspond to the PI phase and the dark regions to the PS. These patterns make clear that the system is microphase separated into three phases and that the PI and PS regions form concentric cylinders.

Concentric Cylindrical Morphology. The results from TEM and SAXS for the chloroform cast SIM-72/77/218 and SIM-72/77/186 samples are given in Figures 1 and 2, respectively. The SAXS pattern suggests the SIM-72/77/218 and SIM-72/77/186 samples exhibit a hexagonal arrangement of microdomains, because the q_n/q_1 values are 1.0: 1.66: 2.59: 2.96 and 1.0: 1.59: 2.63, respectively, which are close to 1: $\sqrt{3}$:($\sqrt{4}$ missing): $\sqrt{7}$:$\sqrt{9}$, which are characteristic for hexagonally packed units. The lowest order d spacings from the SAXS and the unperturbed mean square end-to-end distance for each block are given in Table 2. The SAXS patterns also show that SIM-72/77/218 and SIM-72/77/186 are partially oriented. The arced reflections indicate that the microdomains are predominantly formed

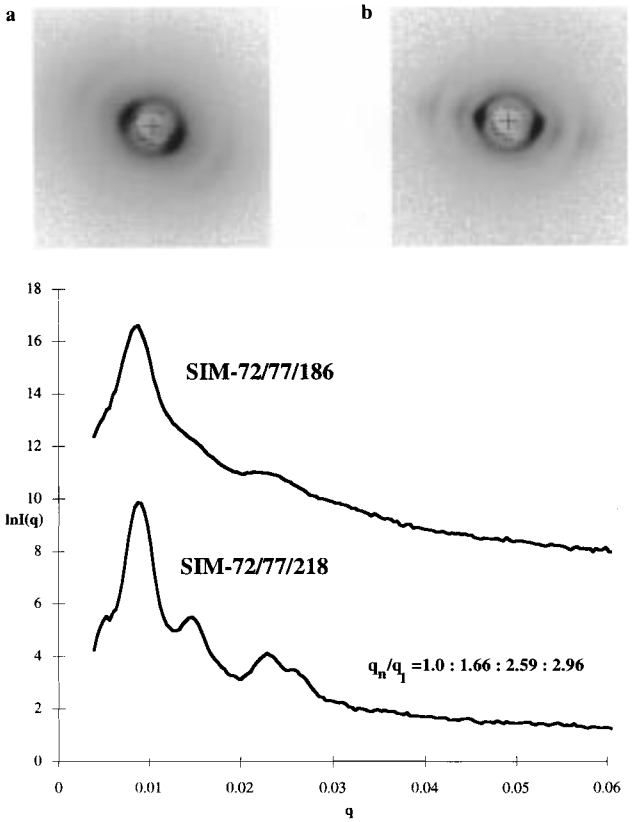

Figure 2. The SAXS patterns of (a) SIM-72/77/186 and (b) SIM-72/77/218. The ratios of the q vectors for the various peaks are given.

Table 2. The Lowest Order *d* Spacings and the Unperturbed Mean Square End-to-End Distance for Each Arm

sample	$\langle R_0^2\rangle^{1/2}$PS (Å)[a]	$\langle R_0^2\rangle^{1/2}$PI (Å)[a]	$\langle R_0^2\rangle^{1/2}$PMMA (Å)[a]	d_1^{SAXS} (Å)
SIM-72/77/218	177	226	304	748
SIM-72/77/186	177	226	281	724
SIM-72/77/144	177	226	247	740
SIM-57/85/49	157	237	144	716

[a] $\langle R_0^2\rangle$ is the unperturbed mean square end-to-end distance for each block calculated from $\langle R_0^2\rangle_i = K_i M_w$.[19]

parallel to the air and substrate surfaces. Hashimoto et al.[18] also noticed partial orientation of microdomains in lamellar and cylindrical block copolymers when simply cast from solution. They attribute the orientation to preferential alignment of the microdomains at the sample−air surface, which influences the transforming solution. This orientation is also confirmed by the TEM images.

Figures 1a and 1c show bright field TEM micrographs of the OsO_4-stained sections. OsO_4 preferentially stains the PI phase, which appears dark, whereas the PS and PMMA phases are not distinguished and appear as a light gray matrix. The microdomain structure is at least biphasic, comprised of hexagonal cylinders of PI in a mixed (or possibly demixed) matrix of PS and PMMA.

To probe the issue of the mixing of the PS and PMMA arms, sections were stained with RuO_4, which is known to preferentially stain PS and slightly stain PI. The TEM micrographs (Figures 1b and 1d) show gray hexagonal cylinders with a dark surrounding annulus in a light gray matrix. This pattern indicates that the PS and PMMA arms do indeed microphase segregate.

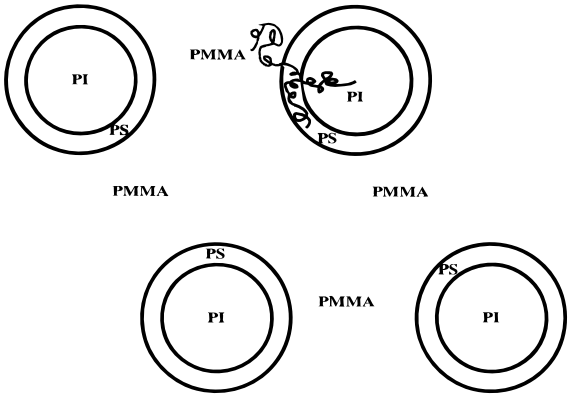

Figure 3. Schematic representation of the microdomain morphology of the SIM-72/77/186 and the SIM-72/77/218 samples, which exhibit hexagonally packed cylinders of PI with a concentric PS annulus in a matrix of PMMA. The chain conformation of the three blocks and the location of the junction point are also presented. The PS and PMMA arms are partially mixed within the PS domain and the junction points are distributed over the PS−PI IMDS.

Combining the two sets of TEM data with the hexagonal packing indicated by SAXS leads to the schematic of the proposed morphology in Figure 3. Note the junction point of the star terpolymer is considered to reside on the PS−PI interface, an arrangement that causes the PMMA chain to penetrate the PS microphase. This notion can be confirmed by calculating the ratio of the outer PS annulus radius (R_2) to the radius of the inner PI cylinder (R_1):

$$R_i = \alpha\sqrt{\frac{\sqrt{3}\phi_i}{2\pi}} \tag{1}$$

where $\phi_i = \phi_{PI}$ for R_1, $\phi_i = \phi_{PI} + \phi_{PS}$ for R_2, and α is the lattice parameter given by the following equation:

$$\alpha = \frac{4\pi}{\sqrt{3}q_{10}} \tag{2}$$

For both SIM-72/77/186 and SIM-72/77/218, the ratio R_2:R_1 is ∼1.35. The experimental ratios measured from the TEM images are ∼1.4 and ∼1.5, respectively. Considering the model shown in Figure 3, because the PMMA chain penetrates the PS phase, the volume fraction for the PS annulus will be somewhat higher and the observed R_2/R_1 values larger than those calculated, as is indeed the case.

The volume fractions of the PS and PI arms of the two samples, SIM-72/77/218 and SIM-72/77/186, differ only by ∼2% and the volume fractions of the PMMA arm differ by ∼4%. This small difference in composition does not lead to a different microstructure for the two samples, as confirmed by both TEM and SAXS.

This kind of concentric cylinder morphology was also observed by Gido et al.[1] in a linear PS−*b*−PI−*b*−P2VP (poly(2-vinyl pyridine)) triblock terpolymer with volume fractions 0.33/0.33/0.33. The TEM images of sections stained with OsO_4 (which preferentially stains the PI) and CH_3I (which preferentially stains the P2VP) exhibited gray central cylindrical cores of P2VP surrounded by a dark shell of PI in a PS matrix. Because there are two junctions in the linear block terpolymer, there was no mixing of one block into the other in the concentric cylindrical morphology.

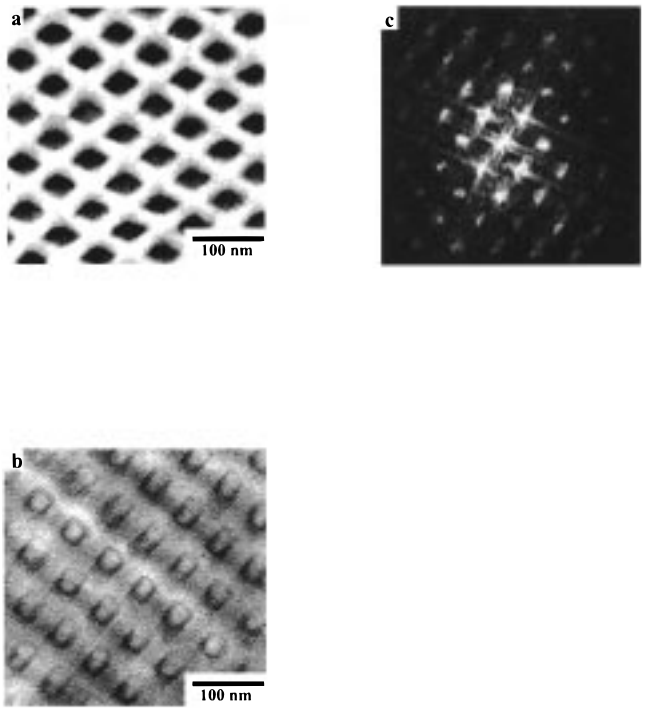

Figure 4. Bright field TEM images of SIM-72/77/144 stained (a) with OsO_4 and (b) with RuO_4. In the OsO_4 stained micrographs, the dark regions correspond to the PI phase, which forms diamond, prism-shape columns, whereas in the RuO_4 stained micrographs, the gray regions correspond to the PI phase and the dark regions to the PS. The copolymers form a three-phase system concentric rhombohedral microdomains of PI and PS. (c) FFT of region a showing Fourier peaks that index to the c2mm plane group.

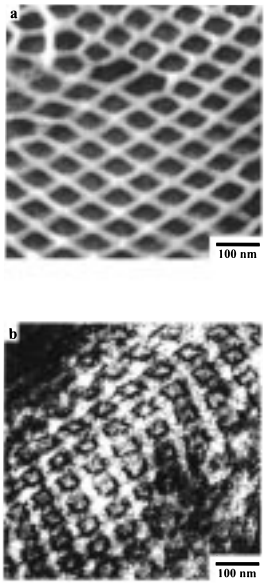

Figure 5. Bright field TEM images of SIM-57/85/49 stained (a) with OsO_4 and (b) with RuO_4. In the OsO_4 stained micrographs, the dark regions correspond to the PI phase that forms rhomboid columns, whereas in the RuO_4 stained micrographs, the gray regions correspond to the PI phase and the dark to the PS phase. The sample thus has a microdomain structure quite similar to SIM-72/77/144.

Concentric Rhombohedral Morphology. Results from TEM for samples SIM-72/77/144 and SIM-57/85/49 are given in Figures 4a−c and 5a and 5b. The respective SAXS patterns are shown in Figure 6. The single, broad, low-angle peak of sample SIM-57/85/49

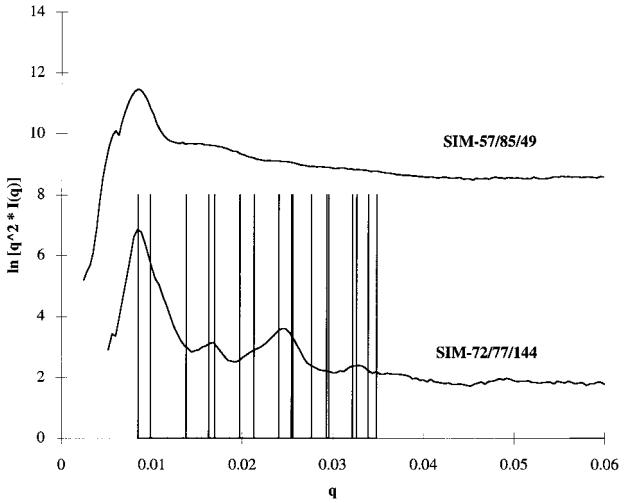

Figure 6. The SAXS patterns of SIM-72/77/144 and SIM-57/85/47.

suggests that while the sample is microphase separated, it does not possess well-defined long-range microdomain ordering. Sample SIM-72/77/144 exhibits four distinct peaks, as well as the indication of several additional peaks by the presence of shoulders on various of the peaks. The q_n/q_1 ratios for the four well-defined peaks are 1.0, 1.95, 2.88 and 3.83, which do not agree with p6mm symmetry.

The advantage of TEM is the ability to select well-ordered grains so that local regions of good microdomain packing can be used to identify the microdomain morphology. Figure 4a, which is an OsO_4 stained section of sample SIM-72/77/144, shows a two-dimensional periodic patterm of diamond-shaped prisms of PI arranged on a centered rectangular lattice. Figure 4b shows another specimen of SIM-72/77/144, which has been stained by RuO_4. Again, diamond-shaped regions are arranged on a centered rectangular lattice, but in this instance, the stained region is localized to an annular region about the PI core. Selected regions from sample SIM-57/85/49 stained with OsO_4 or with RuO_4 show basically the same two-dimensional periodic pattern. Both SIM-72/77/144 and SIM-57/85/49 exhibit periodic stripe patterns in other TEM views consistent with a two-dimensional periodic arrangement of columns. From the TEM micrographs of both SIM-72/77/144 and SIM-57/85/49 the microdomain structure is shown to consist of an inner core region of PI surrounded by a narrow annulus of PS in a matrix of PMMA. The important differences now are that the PI arm does not form hexagonally packed cylinders, and the PI/PS and PS/PMMA surfaces have a rhombohedral shape. Figure 7 gives a schematic representation of the novel morphology emphasizing the non-CMC intermaterial dividing surface (IMDS).

In two dimensions, the conditions to minimize interfacial boundary length at fixed area favors the formation of constant curvature domain boundaries (e.g., straight lines or segments of circular arcs). This inclination is opposed by the tendency for the arms to form domains of optimal and uniform thickness so as to minimize chain deformation energy. When the chain deformation energy is too high, then the system prefers to change the shape of the IMDS. Gido et al.[1] suggested the transition from a CMC IMDS to a non-CMC in a linear ABC triblock could occur when the volume fraction of the coaxial cylinder is larger than ∼0.6 because of the

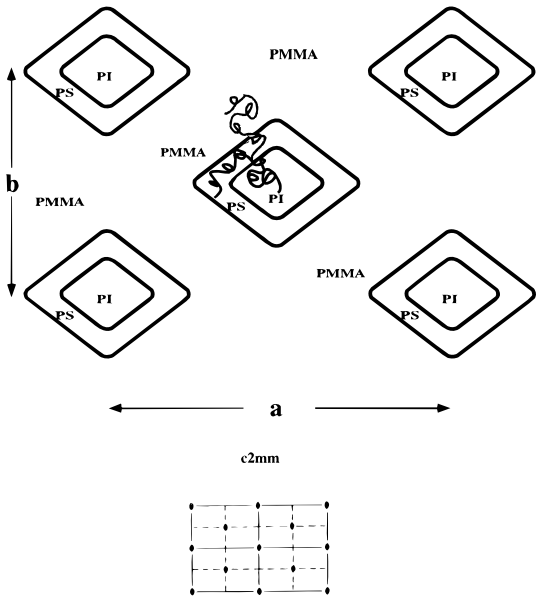

Figure 7. Schematic description of the unit cell for SIM-72/77/144 and SIM-57/85/49 and the symmetry elements of the two-dimensional plane group c2mm: mirror planes (black lines), glide planes (dotted lines), c2 axes (black ellipsoidal objects). Parameters a and b correspond to the lattice parameters of the unit cell (a > b).

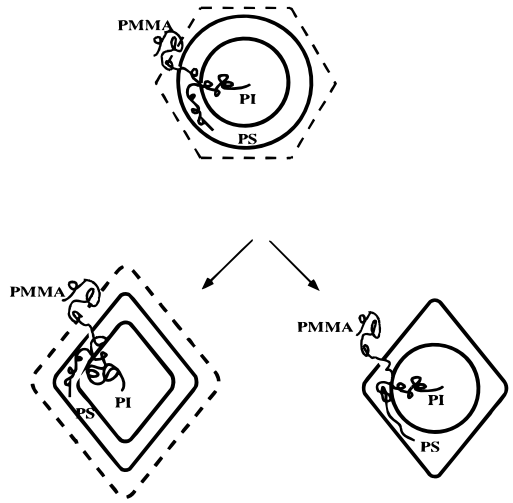

Figure 8. Schematic representation of the morphology of SIM-72/77/144, exhibiting the transition from a CMC intermaterial dividing surface to a non-CMC IMDS. The location of a typical junction point and the chain conformation in each case are also presented.

need to relieve the strong stretching of the relatively short matrix block. The volume fractions in the concentric microdomain columns are 0.56 and 0.78 for the respective copolymers, very high values for a microdomain structure that is not the matrix. The column regions are thus packed unusually close to one another. The IMDS between the PI and PS is also rhombohedral. This result can easily be understood from Figure 8 where for a cylindrically shaped PI microdomain it is evident that the PS chains would have highly variable chain conformations because of the highly variable PS domain thickness. The resultant rhombohedral microstructure is a compromise to both minimize interfacial area and chain stretching.

An FFT analysis of a highly ordered region of SIM-72/77/144 allows the determination of the two-dimensional plane group. From inspection of the forbidden reflections, the two-dimensional plane symmetry group can be determined as c2mm, fulfilling the condition $h + k = 2n$ for allowed reflections. The structure of the rectangular unit cell exhibiting the location of the mirror planes, glide planes, and 2-fold axes is schematically shown in Figure 7.

From inspection of the TEM micrographs of SIM-72/77/144 the ratio of the a axis to the b axis is approximately a/b = 1.4. This permits calculation of the q_n/q_1 ratios for the allowed reflections: 110, 200, 020, 310, 220, 400, 130, 420, 330... as 1.0, 1.16, 1.63, 1.93, 2.0, 2.33, 2.51, 2.84, 3.0, and so on. These peak positions are indicated by the vertical lines on Figure 6. The correspondence between actual peaks and those predicted based upon a 2d periodic structure with plane-group c2mm and a/b = 1.4 is quite reasonable considering the SAXS data is obtained from a much larger sample consisting of small grains with many defects.

A possible scenario for the formation pathway of a PI column surrounded by a PS annulus in a PMMA matrix is the following: Because chloroform is least preferential to the PI component, the first domains to form will be cylinders of PI in a swollen matrix consisting of PS, PMMA, and the solvent. The junction points reside on the cylindrical IMDS. Upon further evaporation, the PS and PMMA will eventually segregate. For SIM-72/77/218 and SIM-72/77/186, the PS forms a "protective" annulus surrounding the hexagonally packed PI cylinders, whereas the majority component PMMA forms the matrix. For SIM-72/77/144 and SIM-57/85/49 PS also tends to form a "protective" annulus. In this case the combined PI and PS domains correspond to a relatively high volume fraction (especially in the case of SIM-57/85/49). The packing of these units deforms them into diamond-shape prisms leading to a change in the shape of both the PI−PS and PS−PMMA interfaces and the change of the arrangement from a hexagonal to a rectangular lattice. Because PMMA segregates last, it forms the matrix even when it is the minority component.

Conclusions

The microdomain morphology of a family of four 3-miktoarm star terpolymers of PS, PI, and PMMA consists of a column of PI surrounded by an annulus of PS in a matrix of PMMA. Instead of two junctions in the case of linear triblocks, there is only one junction for a triblock star. The segment−segment interaction parameters rank as $\chi_{IM} > \chi_{SI} \gg \chi_{SM}$. There is no interface between the two components with the largest χ. The junction points are distributed over the PS−PI IMDS due to partial mixing of the PS and PMMA arms. The architecture of the molecule allows the two most incompatible blocks not to be in contact by forming a "protective" annulus of PS. The low value of χ_{SM} makes it possible for the PMMA block to partially mix into the PS phase and avoid the formation of a microdomain surface between the PI and PMMA arms.

For two of the samples with a total volume fraction of PI and PS of ~0.40, the microdomain structure consists of CMC coaxial cylinders on a two-dimensional hexagonal lattice (plane group symmetry p6mm). For the two terpolymers with a total volume fraction of PI and PS of 0.56 and 0.78, respectively, a novel two-dimensionally periodic non-CMC concentric rhombohedral morphology with plane group symmetry c2mm is observed. This report is the first of a diamond prism-shape IMDS observed in block copolymers.

Acknowledgment. The authors acknowledge support from NSF DMR-9214853. S.S. and N.H. acknowledge the Greek General Secretariat of Research and Technology and the Research Committee of the University of Athens for financial support. We also thank the Center for Materials Science and Engineering at the Massachusetts Institute of Technology for use of the electron microscopy facility. S.S is grateful to Dr. A. Avgeropoulos and Dr. M. Capel for running the SAXS experiments at the National Synchrotron Light Source at Brookhaven National Laboratory.

References and Notes

(1) Gido, S. P.; Schwark, P. W.; Thomas, E. L.; Gonçales, M. C. *Macromolecules* **1993**, *26*, 2636.
(2) Riess, G.; Schlienger, M.; Marti, S. *J. Macromol. Sci., Phys.* **1980**, *B17(2)*, 335.
(3) Auschra, C.; Stadler, R. *Macromolecules* **1993**, *26*, 2171.
(4) Stadler, R.; Auschra, C.; Beckmann, J.; Krappe, U.; Voigt-Martin, I.; Leiber, L. *Macromolecules* **1995**, *28*, 3080.
(5) Junk, K.; Abetz, V.; Stadler, R. *Macromolecules* **1996**, *29*, 1076.
(6) Brinkmann, S.; Stadler, R.; Thomas, E. L. *Macromolecules*, in press.
(7) Mogi, Y.; Nomura, M.; Kotsuji, H.; Ohnishi, K.; Matsushita, Y.; Noda, I. *Macromolecules* **1994**, *27*, 6755.
(8) Nakazawa, H.; Ohta, T. *Macromolecules* **1993**, *26*, 5503.
(9) Zheng, W.; Wang, Z.-G. *Macromolecules* **1995**, *28*, 7215.
(10) Fujimoto, T.; Zhang, H.; Kazanawa, H.; Isono, X.; Hasegawa, H.; Hashimoto, T. *Polymer* **1992**, *33*, 2208.
(11) Hückstädt, H.; Abetz, V.; Stadler, R. *Macromol. Rapid Commun.* **1996**, *17*, 599.
(12) Iatrou, H.; Hadjichristidis, N. *Macromolecules* **1992**, *25*, 4649.
(13) Sioula, S.; Tselikas, Y.; Hadjichristidis, N. *Macromolecules* **1997**, *30*, 1518.
(14) Hadjichristidis, N.; Iatrou, H.; Behal, S. K.; Chludzinski, J. J.; Disko, M. M.; Garner, R. T.; Liang, K. S.; Lohse, D. J.; Milner, S. T. *Macromolecules* **1993**, *26*, 5812.
(15) Okamoto, S.; Hasegawa, H.; Hashimoto, T.; Fujimoto, T.; Zhang, H.; Kazama, T.; Takano, A. *Polymer* **1997**, *38*, 5275.
(16) Capel, M. C.; Smith, G. C.; Yu, B. *Rev. Sci. Instrum.* **1995**, *66*, 2295.
(17) Balsara, N. P. Thermodynamics of Polymer Blends. In *Physical Properties of Polymer Handbook*; Mark, J. E., Ed.; AIP: New York, 1996; Chapter 19.
(18) Hashimoto, T.; Shibayama, M.; Fujimura, M..; Kawai, H. *Block Copolymers. Science and Technology*; Meier, D. J., Ed.; Harwood Academic: 1979; pp 63−108.
(19) Fetters, L. J.; Lohse, D. J.; Richter, D.; Witten, T. A.; Zirkel, A. *Macromolecules* **1994**, *27*, 4639.
(20) Breiner, U.; Krappe, U.; Stadler, R. *Macromol. Rapid Commun.* **1996**, *17*, 567.

MA971848J